Kobe University Repository : Kernel

PDF issue: 2026-11-10

Wide-range work function tuning in gold surfaces modified with fluorobenzenethiols toward application to organic thin-film transistors

Yoshioka, Takumi
Fujita, Hiroki
Kimura, Yoshinari
Hattori, Yoshiaki
Kitamura, Masatoshi

(Citation)
Flexible and Printed Electronics,5(1):014011

(Issue Date)
2020-03

(Resource Type)
journal article

(Version)
Accepted Manuscript

(Rights)
© 2020 IOP Publishing Ltd. This is the Accepted Manuscript version of an article accepted for publication in Flexible and Printed Electronics. IOP Publishing Ltd is not responsible for any errors or omissions in this version of the manuscript or any version derived from it. The Version of Record is available online at…

(URL)
https://hdl.handle.net/20.500.14094/90007472

KOBE UNIVERSITY

Wide-range work function tuning in gold surfaces modified with fluorobenzenethiols toward application to organic thin-film transistors

Takumi Yoshioka, Hiroki Fujita, Yoshinari Kimura, Yoshiaki Hattori, and Masatoshi Kitamura

Department of Electrical and Electronic Engineering, Graduate School of Engineering, Kobe University, Kobe 657-8501, Japan

E-mail: kitamura@eedept.kobe-u.ac.jp

Received xxxxxx
Accepted for publication xxxxxx
Published xxxxxx

Abstract

Surface properties of Au electrodes modified by benzenethiol derivatives with a fluorine atom(s) have been methodically researched based on measurements of the work function and the contact angles. Benzenethiol derivatives with a fluorine atom(s) at ortho, meta, and/or para position were used for modification in this work. The measured work function was in a relatively wide range between 4.24 and 6.02 eV. The work function change from a bare Au surface was explained on the principle of dipole moments obtained by quantum chemical calculation. The water contact angle was found to vary between 64.8° and 97.7°. Furthermore, the surface tension was calculated from the measured contact angles of water and ethylene glycol. The calculated surface tension was reviewed from the perspective of the position of the substitute in the benzenethiol derivative. In addition, organic thin-film transistors (TFTs) with drain and source electrodes modified with 2-fluorobenzenethiol (2-FBT), 3-fluorobenzenethiol (3-FBT) or pentafluorobenzenethiol (PFBT) were characterized as other evaluation of the modified Au surface. The contact resistance in the TFT increased in the order of PFBT, 3-FBT and 2-FBT. The increase of the contact resistance was consistent with the decrease in the work function.

Keywords: benzenethiols, work function, contact angle, organic transistors

1. Introduction

Organic electronic devices such as organic thin-film transistors (TFTs) [1-4] and light-emitting diodes (LEDs) [5-7] have attracted attention because of their application in large area, flexible, lightweight and cost effective devises. In addition, organic TFTs exhibit high field-effect mobilities close to those of oxide TFTs. Field-effect mobilities up to about 10 $cm^2 V^{-1} s^{-1}$ have been reported [8-11]. In an organic TFT with such a high mobility, the interface between the organic semiconductor and the electrode strongly affects its performance. The contact resistance at the interface is known to suppress the overall performance. The difference in energy level between the contact metal and the organic semiconductor typically cause a large contact resistance at its interface.

For organic TFTs, contact metals covered with a specific monolayer has been used to control the work function [12-17]. The dipole moment within the monolayer leads to a change in the work function. Benzenethiol derivatives have

 © xxxx IOP Publishing Ltd

been used for such surface modification. Pentafluorobenzenethiol (PFBT) [18,19] and 4-fluorobenzenthiol (4-FBT) [19-21] have been used to increase the work function of the contact electrodes in p-channel organic TFTs. In particular, PFBT are currently used by many research groups [22-24]. Conversely, 4-methylbenzenethiol (MBT) [25-27] and 4-(dimethylamino)benzenethiol (DABT) [25,28] have been used to decrease the work function of the contact electrodes in n-channel organic TFTs. Although these four benzenethiol derivatives are examples used in surface modification, in most cases, derivatives with a substituent at para position and no substituent at either the ortho and meta position have been used for surface modification in organic TFTs (excluding PFBT).

In surface modification, the degree of work function change depends on the dipole moment of a benzenethiol derivative. The substituent in a benzenethiol derivative induces the dipole moment and strongly affects the surface energy on the monolayer formed by the benzenethiol derivative [29-33]. The Au surfaces modified with PFBT, 4-FBT, and MBT, which are used for organic TFTs, have relative low surface tensions, and exhibit large water contact angles [17]. The surface energy plays an important role in the solution process in which an organic layer is coated from a solvent containing the organic molecule. The surface with a low surface tension is not suitable for solution process of organic semiconductor for organic TFTs [34-36]. If a benzenethiol derivative with a substituent at para position is used for surface modification, it is challenging to control both the work function and the surface energy, independently. If a benzenethiol derivative with a substituent(s) at ortho and/or meta position is used for surface modification, the degree of freedom in manipulating the surface properties is increased. It is possible that such a surface modification improves the characteristics of organic TFTs fabricated from solution process.

In this paper, we report on the work function and surface tension of a Au surface modified with benzenethiol derivatives having a fluorine atom(s). The measured work function is reviewed on the principle of dipole moments calculated by density functional theory (DFT). The surface tension was calculated from contact angles of water and ethylene glycol droplets on a modified surface. Finally, the characteristics of organic TFTs with modified electrodes are represented in an application for modified electrodes.

2. Molecules used for modification

The following benzenethiol derivatives having a fluorine atom(s) were used for surface modification: 2-fluorobenzenethiol (2-FBT), 3-fluorobenzenethiol (3-FBT), 4-fluorobenzenethiol (4-FBT), 2,6-difluorobenzenethiol (2,6-DFBT), 3,5-difluorobenzenethiol (3,5-DFBT), 3,4,5-trifluorobenzenethiol (TFBT), pentafluorobenzenethiol (PFBT), and 2,3,5,6-tetrafluoro-4-(trifluoromethyl)benzene-thiol (TMBT). The molecular structure of each is shown in figure 1(a). 2-FBT, 3-FBT, and 4-FBT are useful in evaluating the impact of the fluorine atom at the ortho, meta, and para position of the benzene ring, on the work function and surface tension, respectively. The combinations of either 2-FBT and 2,6-DFBT, or 3-FBT and 3,5-DFBT are useful to examine the impact that the number of fluorine atoms has. PFBT is most commonly used for surface modification on drain and source electrodes of bottom-contact p-channel organic TFTs. This is because a Au surface modified by PFBT has a relative high work function when compared to Au surfaces that have been modified by other benzenethiol derivatives [16,17]. However, a fluorine atom at the ortho position possibly causes a decrease in the work function. To confirm this, TFBT with no fluorine atom at the ortho position was selected. Similarly, a derivative with a group containing multiple fluorine atoms at the para position possibly contributes to an increase in the work function. To confirm this, TMBT with a trifluoromethyl group at the para position was selected. It is expected that Au surfaces modified by TFBT and TMBT have higher work functions than when modified by PFBT.

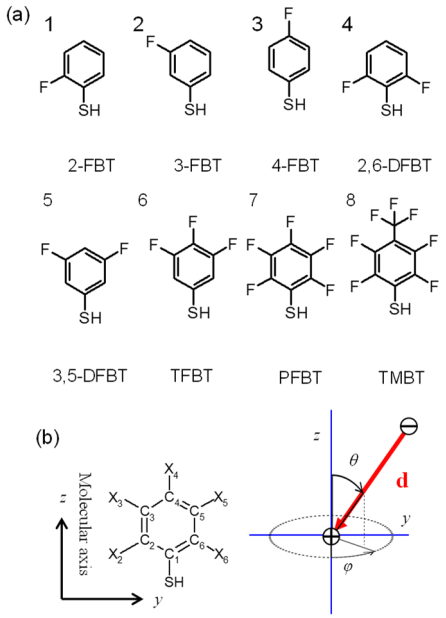

Figure 1. (a) Chemical structures of benzenethiol derivatives used for surface modification. (b) Coordinate system for expressing the molecule axis and the direction of a dipole moment.

The dipole moment **d** for the molecules shown in figure 1(a) was calculated to deliberate work functions of modified Au surfaces. Dipole moments can be obtained from quantum chemical calculations. In this study, a quantum chemical calculation was performed on the principle of DFT, using Gaussian 09 software, with the B3LYP method, and the

Table 1 Magnitude of dipole moment |**d**|, the *z*-component d_z, the polar angle θ, and measured work function Φ.

Molecule	|**d**| (D)	d_z (D)	θ (degree)	Φ (eV)
2,6-DFBT	2.84	−2.62	157.1	4.24
2-FBT	2.02	−1.86	157.2	4.36
Bare	–	–	–	4.97
3-FBT	0.95	0.20	77.6	4.96
4-FBT	1.35	0.72	57.8	5.22
3,5-DFBT	1.48	0.89	52.7	5.20
PFBT	2.35	2.08	28.1	5.73
TFBT	3.24	3.01	21.3	5.91
TMBT	3.99	3.75	20.0	6.02

LanL2DZ basis set [34]. The calculated dipole moments are summarized in table 1 and the measured work functions are explained in section 3. The dipole moments are denoted by debye (D) unit. The direction of **d** does not correspond with the molecular axis shown in figure 1(b), and therefore the polar angle θ for **d** is typically not equal to 0° or 180° in spherical coordinate system. Conversely, the azimuth angle φ for **d** is approximately equal to 0°, 90°, 180°, or 270°. The *z*-component (d_z) of **d** defined as $d_z = |\mathbf{d}| \cos\theta$, affects change in the work function. Thus, θ and d_z values obtained are also shown in table 1.

The calculated d_z values range between −2.62 and +3.75 D. Dipole moments for 2-FBT, 3-FBT, and 4-FBT have θ values of 157.2°, 77.6° and 57.8°, respectively. The different in θ leads to large variation in d_z. In particular, a fluorine atom at the ortho position leads to a negative d_z. Also, the dipole moment for 2,6-DFBT indicates that two fluorine atoms at the ortho position contribute to more negative d_z. TFBT and TMBT have larger d_z than PFBT, which was expected. This indicates that fluorine atoms at the ortho positions of PFBT suppress the magnitude of d_z.

3. Work function measurement

Figure 2(a) is a schematic illustration of a Au layer modified with a benzenethiol derivative, prepared for measuring the work function and the contact angle. A monolayer, formed on a metal surface from a molecule with **d,** induces a potential energy shift. This can be observed from a change in the work function of the modified metal, as shown in figure 2(b). The work function change $\Delta\Phi$ can be given by

$$\Delta\Phi = \frac{qN|\mathbf{d}|\cos\alpha}{\varepsilon} \quad (1)$$

where q is the elementary charge, N is the area density of the molecule, α is the angle of the dipole direction relative to the surface normal, and ε is the permittivity of the monolayer [38]. When the positive (negative) charge of the dipole is placed on the surface, cos α is positive (negative) and the dipole induces an increase (a decrease) of the work function.

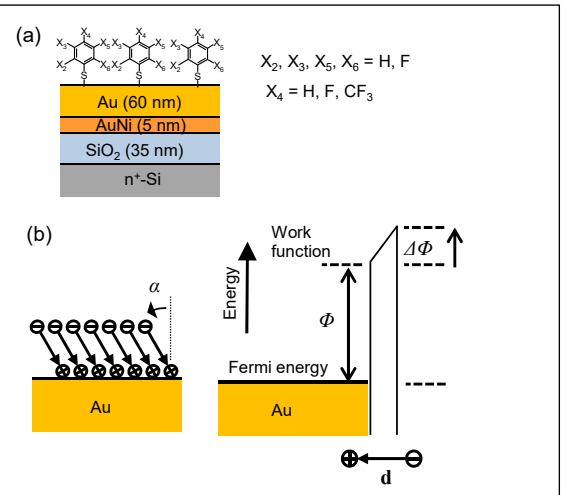

Figure 2. (a) Schematic illustration of a Au surface modified with a benzenethiol derivative evaluated in this study. (b) Energy diagram for a Au surface covered with a monolayer consisting of molecules having a dipole moment **d**.

The substrate with a modified Au surface was prepared as follows. The 5 nm thick adhesive $Au_{0.95}Ni_{0.05}$ and the 60 nm thick Au layers were deposited by thermal evaporation at room temperature on a n^+-Si substrate with 35 nm thick SiO_2. The substrate was cleaned in ethanol, and was exposed to UV/ozone to remove carbon contaminations. To form a monolayer, the substrate was immersed for 5 min in a 10 mmol/L ethanol solution containing a benzenethiol derivative. At this concentration, the immersion time is enough to saturate the area density of the molecule [16, 39]. After the monolayer was formed, the substrate was rinsed with ethanol several times. A substrate rinsed with ethanol without monolayer formation after UV/ozone treatment was used as a bare Au substrate. The resulting substrate was used for measurement of the work function and the contact angle. The work function was measured with an atmospheric photoelectron spectrometer (Riken Keiki AC-2).

Figure 3(a) shows the electron emitting yields measured for Au surfaces modified with 2-FBT, 3-FBT, and PFBT as examples of work function measurement. The square root of electron emitting yields increases almost linearly above a certain photon energy. The work function is obtained from the energy of the intersection of the baseline and line fitting to plots increasing linearly, as shown in figure 3(a). The arrows show the work functions estimated from the fitting. Figure 3(b) shows the measured Φ versus d_z for Au surfaces modified with the molecules in figure 1(a). The measured Φ values are listed in table 1. The dotted line in figure 3(b) is a line fitting to the plots of Φ versus d_z and can be represented by $\Phi(d_z)$ = (0.301 eV/D) d_z + 4.972 eV. The plots are nearly on the dotted line. In addition, $\Phi(0)$ = 4.972 eV is very close

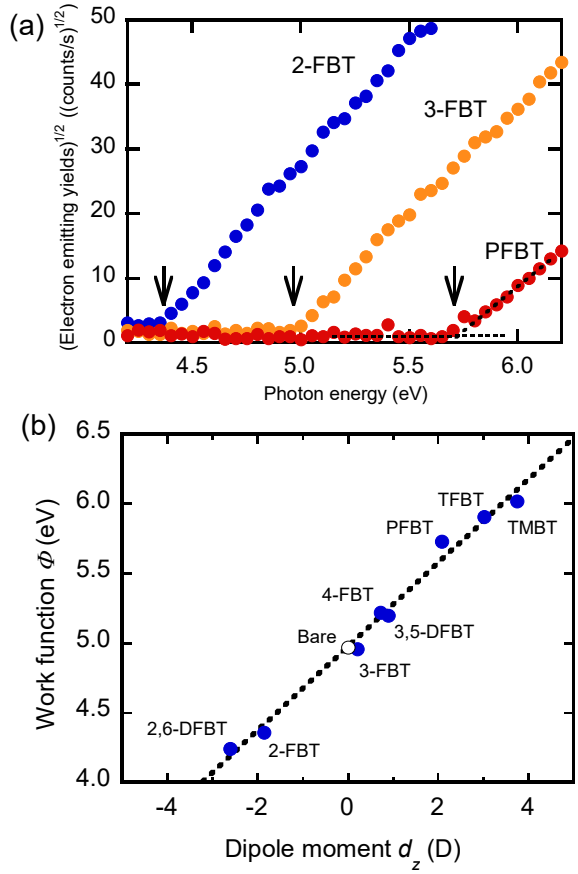

Figure 3. (a) Electron emitting yields versus photon energy for PFBT-, 3-FBT-, and 2-FBT-modified Au surfaces measured with an atmospheric photoelectron spectrometer. (b) Measured work functions of Au surfaces modified with various benzenethiol derivatives (blue filled circles) and that of a bare Au surface (open circle). The horizontal axis is represented by the *z*-component d_z of dipole moments calculated for molecules used for the surface modification.

to a work function of 4.97 eV measured for a bare Au surface. This indicates that the work function change $\Delta\Phi$ is proportional to d_z. This suggests that the area density of the molecule in a monolayer does not largely depend on the type of benzenethiol derivative. Assuming that the molecular axis is perpendicular to the surface, α in equation (1) is equal to the polar angle θ of the dipole moment and $|\mathbf{d}| \cos\alpha = |\mathbf{d}| \cos\theta = d_z$. In this case, $qN/\varepsilon = 0.301$ eV/D. Thus, the N values are estimated to be 2.4×10^{14} cm^{-2} by assuming that $\varepsilon = 3.0$ [40, 41]. The atomic density on a Au(111) surface is calculated from the lattice constant to be about 1.38×10^{15} cm^{-2}. The N values for the benzenethiol derivatives suggest that a molecule for formation of a monolayer is present on a surface area consisting of approximately six Au atoms.

The measured Φ values are between 4.24 and 6.02 eV. The TMBT-modified Au surface exhibits the highest work function of 6.02 eV and the 2,6-DFBT exhibits the lowest work function of 4.24 eV. Since the experimental $\Delta\Phi$ is proportional to the calculated d_z, the work function agrees with the result expected from the dipole moment. Thus, the anticipated value of the measured Φ coincides with the estimations of each benzenethiol derivative as described in section 2. As predicted in section 2, the use of 2,6-DFBT with two fluorine atoms at the ortho positions is useful to decrease the work function of a modified metal surface. We have reported on the work function of Au surfaces modified with various benzenethiol derivatives [16,17,33]. The DABT-modified Au surface has exhibited the lowest work function of 4.37 eV [17]. The work function of 2,6-DFBT, 4.24 eV, is lower than that of DABT. The use of a 2,6-DFBT-modified Au surface could possibly improve the characteristics of n-channel organic TFTs with bottom-contact configuration.

4. Contact angle measurement

Figure 4(a) shows a schematic illustration of the setup to measure the contact angle. De-ionized water and ethylene glycol were used in the measurements. An image of a droplet on a substrate was captured with a digital microscope and used to measure the size of the droplet. The contact angle θ_C on a substrate was calculated using the following equation:

$$\theta_C = 2\tan^{-1}(2h/l) \qquad (2)$$

where h and l are the height and the baseline length of the droplet on the substrate. The θ_C value in this paper is an average of values calculated from contact angles measured at three or more points on a substrate. To demonstrate contact-angle measurement, microphotographs of water droplets on Au surfaces modified with 2-FBT and TMBT are shown in figure 4(b) and 4(c), respectively. The contact angles are 64.8° for 2-FBT and 97.7° for TMBT. The contact angle adopted in this study is a static contact angle, and probably different from the dynamic contact angle [42]. Although dynamic contact angle play an important role in solution

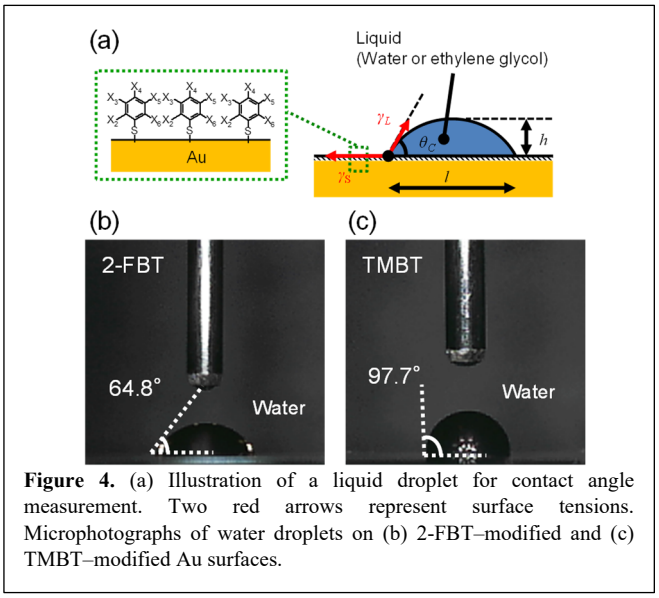

Figure 4. (a) Illustration of a liquid droplet for contact angle measurement. Two red arrows represent surface tensions. Microphotographs of water droplets on (b) 2-FBT–modified and (c) TMBT–modified Au surfaces.

Table 2 Contact angle of water (θ_W) and ethylene glycol (θ_{EG}) measured on Au surfaces modified with various benzenethiol derivatives; dispersion (γ_S^d) and polar (γ_S^p) components of surface tension (γ_S) calculated from the measured contact angle. The value after ± indicates the standard deviation.

	Contact angle (degree)		Surface tension (mN/m)		
	θ_W	θ_{EG}	γ_S^d	γ_S^p	γ_S
Bare	57.1±1.61	-	-	-	-
2-FBT	64.8±0.76	43.8±3.27	14.9±2.75	22.7±2.50	37.6±0.64
2,6-DFBT	67.7±0.46	45.1±2.30	16.7±2.09	19.0±1.60	35.8±0.61
3-FBT	77.4±0.75	50.4±1.77	22.8±2.21	9.5±1.16	32.3±1.18
3,5-DFBT	78.1±0.60	52.2±1.77	21.6±2.11	9.7±1.11	31.2±1.08
4-FBT	85.1±1.91	55.1±0.34	27.4±2.76	4.5±1.47	31.9±1.30
TFBT	89.5±2.25	60.3±0.67	26.7±3.35	3.2±1.42	30.0±1.96
PFBT	88.6±0.59	61.7±0.55	23.6±1.06	4.1±0.48	27.7±0.62
TMBT	97.7±4.94	69.2±0.95	25.7±6.82	2.0±2.22	27.7±4.76

process for organic TFTs, we simply focus on static contact angles as the first research of derivatives listed in figure 1.

The contact angle is expressed as

$$1+\cos\theta_C = 2\sqrt{\gamma_S^{\,d}}\,\frac{\sqrt{\gamma_L^{\,d}}}{\gamma_L} + 2\sqrt{\gamma_S^{\,p}}\,\frac{\sqrt{\gamma_L^{\,p}}}{\gamma_L} \qquad (3)$$

where γ_L is the interfacial tension for the liquid-air interface, γ_L^d is the dispersion component of γ_L, γ_L^p is the polar component of γ_L, γ_S^d and γ_S^p are respectively the dispersion and polar components of the interfacial tension for the solid-air γ_S [43-45]. Using contact angles measured for water (θ_W) and for ethylene glycol (θ_{EG}), γ_S^d and γ_S^p can be calculated from equation (3). In this study, γ_L^d = 22.1 mN/m, γ_L^p = 50.7 mN/m for water and γ_L^d = 30.1 mN/m, and γ_L^p = 17.6 mN/m for ethylene glycol were used in the calculations [44].

The measured contact angles and calculated surface tensions on the Au surfaces modified with the various benzenethiol derivatives are listed in table 2 in descending order of γ_S and depicted in figure 5. The θ_W values for modified Au surfaces range from 64.8° to 97.7°, which is higher than that of a bare Au surface. The highest value of θ_W = 97.7° was obtained from the TMBT-modified Au surface. The second highest value of θ_W = 89.5° was obtained from the TFBT-modified Au surface. The value for TFBT is close to that for PFBT-modified Au surface, suggesting that fluorine atoms at meta and para positions are dominant at a high contact angle. Conversely, the θ_W value for 2,6-DFBT is slightly higher than that for 2-FBT. It seems that a fluorine atom at an ortho position slightly affects a high contact angle. The ascending order of θ_W is almost the same as that of θ_{EG}. We have reported θ_W values of Au surfaces modified with various benzenethiol derivatives [17,33]. The θ_W value ranged between 77.5° and 88.3°, except for benzenethiol derivatives containing O or N atoms. The results in table 2 suggest that the use of benzenethiol derivatives examined in this study expands the range of θ_W.

The γ_S values calculated are in the range of 26.8 and 37.4 mN/m, as indicated in table 2. As predicted from the measured water contact angles, the TMBT- and 2-FBT-modified Au surfaces have the lowest and the highest surface tensions, respectively. In general, fluorine atoms lead to low surface energy.

We have reported that a MBT-modified Au surface has Φ = 4.47 eV and θ_W = 88.3° [33]. The Φ = 4.47 eV for MBT is close to Φ = 4.36 eV for 2-FBT-modified Au surface in this study. On the other hand, the 2-FBT-modified Au surface exhibited θ_W = 64.8°, which is far from θ_W = 88.3° for MBT. The relative low contact angle of 2-FBT is attributed to the high surface tension. Au electrodes modified with 2-FBT is

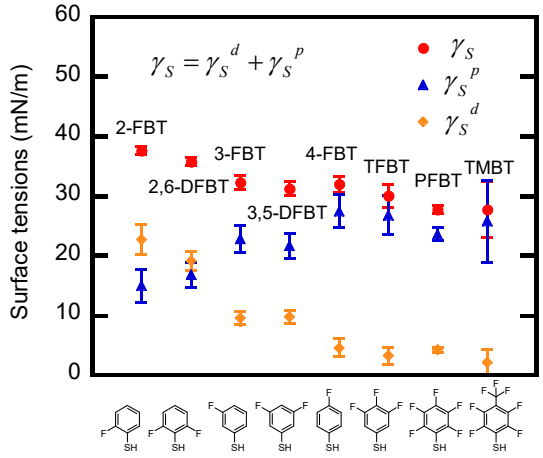

Figure 5. Surface tension γ^S (red filled circles), dispersion component γ_S^d (orange filled diamonds) and polar component γ_S^p (blue filled triangles) of Au surfaces modified with various benzenethiol derivatives. The length of the error bar is twice the standard deviation.

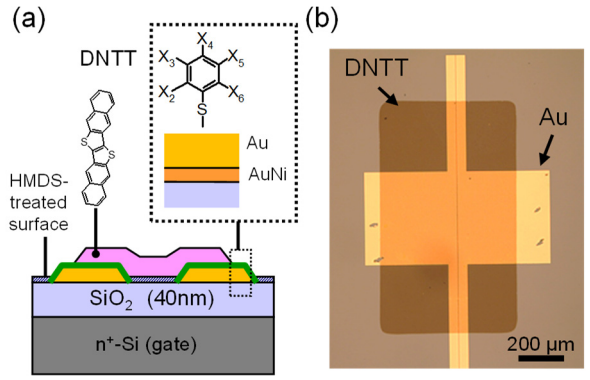

Figure 6. (a) Cross-sectional illustration of a DNTT TFT having electrodes modified with a benzenethiol derivative. (b) Photograph of a fabricated DNTT TFT with L = 2 μm.

suitable for organic TFTs fabricated from solution process. The use of a benzenethiol derivative having a substituent at an ortho position allows us to select surfaces with a certain work function and different water wettability.

5. Application to organic thin-film transistors

Organic TFTs were fabricated for the evaluation of modified electrodes. PFBT, 3-FBT, and 2-FBT were used for surface modification of the contact electrode. Figure 6(a) shows the cross-section of a fabricated TFT. Dinaphtho[2,3-b:2',3'-f]thieno[3,2-b]thiophene (DNTT) was used as the channel material. The highest occupied molecular orbital energy level of a DNTT molecule has been calculated to be −5.19 eV using a quantum chemical calculation [46]. The DNTT TFT was fabricated on a highly-doped n-type silicon substrate (n^+-Si) with a 40 nm thick SiO_2 having a unit area capacitance of 83.2 nF/cm^2. Drain and source electrodes were patterned by conventional photolithography and lift-off process. The 5 nm thick $Au_{0.95}Ni_{0.05}$ adhesive layer and the 25 nm thick Au layer were deposited by thermal evaporation. The use of AuNi as an adhesive layer contributes to lowering of contact resistance [47]. The substrate surface was treated by UV/ozone, and exposed to a hexamethyldisilazane (HMDS) vapor. For the HMDS treatment, the substrate was heated at 120 °C for about 1 h. As a result, a trimethylsilyl monolayer was formed on the SiO_2 surface. For the formation of a monoleyar on the drain and source electrodes, the substrate was immersed for 5 min in a 10 mmol/L acetonitrile solution with PFBT, 3-FBT, or 2-FBT. Finally, the 30 nm thick DNTT was deposited through a shadow mask at room temperature. The channel width (W) was 1 mm and, the channel length (L) was 2, 4, 10, 20, or 40 μm. The photograph of a DNTT TFT is shown in figure 6(b). The fabricated transistors were electrically characterized at room temperature in a dry-nitrogen filled glovebox.

Figure 7(a) shows the drain current (I_D) versus gate voltage (V_G) characteristics at a drain voltage of (V_D) of −15 V for TFTs with L = 4 μm. The field-effect mobilities in the saturation regime (μ_{sat}) were estimated from the transfer curves to be 0.56 cm^2 V^{-1} s^{-1} for PFBT, 0.44 cm^2 V^{-1} s^{-1} for 3-FBT, and 0.25 cm^2 V^{-1} s^{-1} for 2-FBT. The threshold voltages (V_T) were −2.1 V for PFBT, −2.8 V for 3-FBT, and −3.0 V for 2-FBT. The μ_{sat} value decreases in the order of PFBT, 3-FBT, and 2-FBT. The field-effect mobilities in the linear regime were estimated from the transfer curves at V_D = −1 V (not shown) to be 0.11 cm^2 V^{-1} s^{-1} for PFBT, 0.036 cm^2 V^{-1} s^{-1} for 3-FBT, and 0.017 cm^2 V^{-1} s^{-1} for 2-FBT. The decrease in mobility in the linear regime is noticeable when compared to those in the saturation regime. The decrease seems to reflect the difference in the contact resistance at the interface between the DNTT and the modified Au.

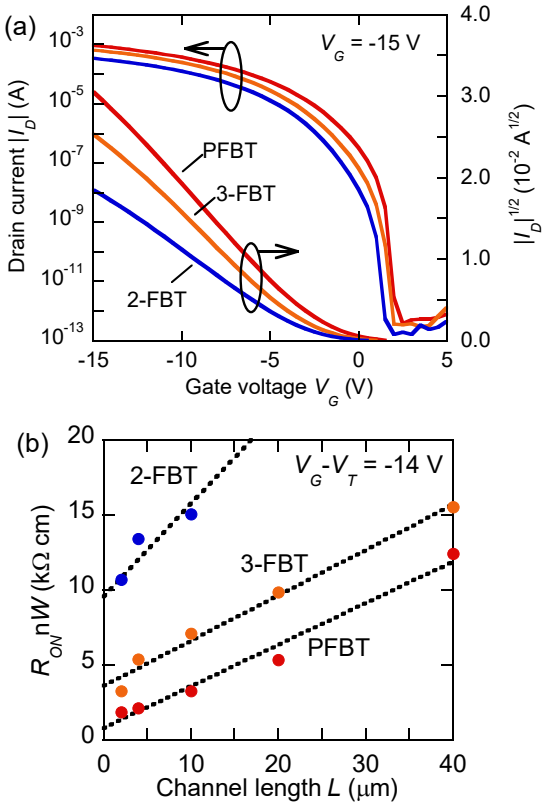

Figure 7. (a) I_D-V_G and $|I_D|^{1/2}$-V_G characteristics at V_D = −15 V for DNTT TFTs of L = 4 μm having electrodes modified with PFBT, 3-FBT, and 2-FBT. (b) Normalized on resistance versus channel length measured at V_G−V_T = −14 V and V_D = −1 V for DNTT TFTs having electrodes modified with PFBT, 3-FBT, and 2-FBT used for calculation of contact resistance.

Therefore, the contact resistance (R_C) was examined by the transfer line method in which R_C is calculated from the channel-length dependence of on-resistance: $R_{ON} = 1(\partial I_D/\partial V_D)$. Figure 7(b) shows the width-normalized R_{ON} versus L of organic TFTs with PFBT-, 3-FBT-, and 2-FBT-modified electrodes. The contact resistance is obtained as the value of R_{ON} at L = 0. The contact resistances for PFBT, 3-FBT, and 2-FBT were estimated to be 0.84, 3.7, and 9.6 kΩ

cm, respectively. As anticipated from the current-voltage characteristics, the contact resistance increases in the order of PFBT, 3-FBT, and 2-FBT. The increase is possibly attributed to the decrease in work function in the same order. The measured work functions of PFBT-, 3-FBT-, and 2-FBT-Au surfaces given in table 1 were 5.73, 4.96, and 4.36 eV, respectively. Also, the difference in the surface tension of the modified electrodes may cause the different in the contact resistance. High surface tension is more suitable to improve the characteristics of organic TFTs. The contact resistance for Au electrodes modified with 2-FBT is large despite the high surface tension. Thus, the large contact resistance for 2-FBT is mainly due to the low work function of the Au electrodes modified with 2-FBT. A modified metal with a low work function is not suitable for drain and source electrodes in p-channel organic TFT, organic TFTs with such a modified electrode with a low function were fabricated to examine the influence of the work function change in this study. Conversely, use of TFBT- or TMBT-modified electrodes may reduce the contact resistance and improve the transistor performance.

6. Conclusion

We investigated the surface properties of Au surfaces modified with benzenethiol derivatives having a fluorine atom(s) by measuring the work function and the contact angles. The work function measured was in the wide range of 4.24 to 6.02 eV, and increased almost linearly with the *z*-component of the dipole moment in the benzenethiol derivative that was used for the modification. The work functions of TFBT- and TMBT-modified Au surfaces were 5.91 and 6.02 eV, respectively, which are higher than that of a PFBT-modified Au surface. The water contact angle was found to vary in the wide range of 64.8 to 97.7°. Also, the surface tension was in the wide range of 26.8 to 37.4 mN/m. The use of a benzenethiol derivative with a substituent(s) at an ortho position(s) expanded the range of water contact angle and surface tension. The work function measured and the wettability observed for the modified Au surfaces appear relevant in the design of electronic devices with metals that are modified with benzenethiol derivatives.

Acknowledgements

This work was supported by JSPS KAKENHI Grant Number 19H02171, 19K15048, and 17H06229. The authors would like to thank Nippon Kayaku Co., Ltd. for supplying us DNTT. The authors would like to thank Enago (www.enago.jp) for the English language review.

ORCID iDs

Masatoshi Kitamura https://orcid.org/0000-0003-1342-4796

References

[1] Taylor D M 2016 Progress in organic integrated circuit manufacture *J. Appl. Phys.* **55** 02BA01

[2] Fukuda K, Takeda Y, Yoshimura Y, Shiwaku R, Tran L T, Sekine T, Mizukami M, Kumaki D and Tokito S 2014 Fully-printed high-performance organic thin-film transistors and circuitry on one-micron-thick polymer films *Nat. Commun.* **3** 1259

[3] Yi H T, Payne M M, Anthony J E and Podzorov V 2014 Ultra-flexible solution-processed organic field-effect transistors *Nat. Commun.* **5** 4147

[4] Sekitani T and Someya T 2012 Ambient Electronics *Jpn. J. Appl. Phys.* **51** 100001

[5] Adachi C 2014 Third-generation organic electroluminescence *Jpn. J. Appl. Phys.* **53** 060101

[6] Kalyani N T and Dhoble S J 2012 Organic light emitting diodes: Energy saving lighting technology — A review *Renew. Sust. Energy Rev.* **16** 2696-723

[7] Ho S, Liu S, Chen Y and So F 2015 Review of recent progress in multilayer solution-processed organic light-emitting diodes *J. Photonics Energy* **5** 057611

[8] Watanabe Y, Sasabe H and Kido J 2019 Review of molecular engineering for horizontal molecular orientation in organic light-emitting devices *Bull. Chem. Soc. Jpn.* **92** 716-28

[9] Kang M J, Doi I, Mori H, Miyazaki E, Takimiya K, Ikeda M and Kuwabara H 2011 Alkylated dinaphtho[2,3- b :2',3'- f]thieno[3,2-b]thiophenes(Cn-DNTTs): Organic semiconductors for high-performance thin-film transistors *Adv. Mater.* **23** 1222-5

[10] Kanayama K, Hirose Y, Soeda J, Yoshizumi M, Uemura T, Uno M, Li W, Kang M J, Yamagishi M, Okada Y, Miyazaki E, Nakazawa Y, Nakao A, Takimiya K and Takeya J 2011 Patternable solution-crystallized organic transistors with high charge carrier mobility *Adv. Mater.* **23** 1626-9

[11] Minemawari H, Yamada T, Matsui H, Tsutsumi J, Haas S, Chiba R, Kumai R and Hasegawa T 2011 Inkjet printing of single-crystal films *Nature* **475** 364-7

[12] He K, Li W, Tian H, Zhang J, Yan D, Geng Y and Wang F 2017 Asymmetric conjugated molecules based on [1]Benzothieno[3,2‑b][1]benzothiophene for high-mobility organic thin-film transistors: Influence of alkyl chain length *ACS Appl. Mater. Interfaces* **9** 35427-36

[13] Evans S D and Ulman A 1990 Surface potential studies of alkyl-thiol monolayers adsorbed on gold *Chem. Phys. Lett.* **170** 462-6

[14] Campbell I H, Rubin R, Zawodzinski T A, Kress J D, Martin R L, Smith D L, Barashkov N N and Ferraris J P 1996 Controlling schottky energy barriers in organic electronic devices using self-assembled monolayers *Phys. Rev.* B **54** 14321-4

[15] Boudinet D, Benwadih M, Qi Y, Altazin S, Verilhac J-M, Kroger M, Serbutoviez C, Gwoziecki R, Coppard R, Le Blevennec G, Kahn A and Horowitz G 2010 Modification of gold source and drain electrodes by self-assembled monolayer in staggered n- and p-channel organic thin film transistors *Org. Electron.* **11** 227-37

[16] Kuzumoto Y and Kitamura M 2014 Work function of gold surfaces modified using substituted benzenethiols: Reaction

time dependence and thermal stability *Appl. Phys. Express* **7** 035701
[17] Tatara S, Kuzumoto Y and Kitamura M 2016 Surface properties of substituted-benzenethiol monolayers on gold and silver: Work function, wettability, and surface tension *Jpn. J. Appl. Phys.* **55** 03DD02
[18] Park S K and Jackson T N 2007 High mobility solution processed 6,13-bis(triisopropyl-silylethynyl) pentacene organic thin film transistors *Appl. Phys. Lett.* **91** 063514
[19] Hong J-P, Park A-Y, Lee S, Kang J, Shin N and Yoon D Y 2008 Tuning of Ag work functions by self-assembled monolayers of aromatic thiols for an efficient hole injection for solution processed triisopropylsilylethynyl pentacene organic thin film transistors *Appl. Phys. Lett.* **92** 143311
[20] Xie Y, Cai S, Shi Q, Ouyang S, Lee W-Y, Bao Z, Matthews J R, Bellman R A, He M and Fong H H 2014 High performance organic thin film transistors using chemically modified bottom contacts and dielectric surfaces *Organic Electron.* **15** 2073-8
[21] Xie X Y, Ouyang S-H, Wang D-P, Zhu D-L, Xu X, Te T and F H-H 2015 Performance improvement in polymeric thin film transistors using chemically modified both silver bottom contacts and dielectric surfaces *Chin. Phys.* B **24** 096803
[22] Youn J, Dholakia G R, Huang H, Hennek J W, Facchetti A and Marks T J 2012 Influence of thiol self-assembled monolayer processing on bottom-contact thin-film transistors based on n-type organic semiconductors *Adv. Funct. Mater.* **22** 1856-1869
[23] Kitamura M, Kuzumoto Y, and Arakawa Y 2013 Short-channel, high-mobility organic thin-film transistors with alkylated dinaphthothienothiophene *Phys. Status Solidi* C **10** 1632-5
[24] Bok M, Jeong J-H, and Lim E 2019 Carrier behaviors of 6,13-Bis (triisopropylsilylethynyl) pentacene device with self-assembled monolayer *Mater. Chem. Phys.* **227** 250-4
[25] Kitamura M, Kuzumoto Y, Aomori S, Kamura M, Na J H and Arakawa Y 2009 Threshold voltage control of bottom-contact n-channel organic thin-film transistors using modified drain/source electrodes *Appl. Phys. Lett.* **94** 083310
[26] Kitamura M, Kuzumoto Y, Aomori S and Arakawa Y 2011 High-frequency organic complementary ring oscillator operating up to 200 kHz *Appl. Phys. Express* **4** 051601
[27] Takeda Y, Hayasaka K, Shiwaku R, Yokosawa K, Shiba T. Mamada M, Kumaki D, Fukuda K and Tokito S 2016 Fabrication of ultra-thin printed organic TFT CMOS logic circuits optimized for low-voltage wearable sensor applications *Sci. Rep.* **6** 25714
[28] Robin M, Harnois M, Molard Y and Jacques E 2016 Improvement of n-type OTFT electrical stability by gold electrode modification *Org Electron.* **39** 214-21
[29] Ulman A, Evans S D, Shnidman Y, Sharma R, Eilers J E and Chang J C 1991 Concentration-driven surface transition in the wetting of mixed alkanethiol monolayers on gold *J. Am. Chem. Soc.* **113** 1499-1506
[30] Lee S, Puck A, Graupe M, Colorado R, Shon Y-S, Lee T R and Perry S S 2001 Structure, wettability, and frictional properties of phenyl-terminated self-assembled monolayers on gold *Langmuir* **17** 7364-70
[31] Baralia G G, Duwez A-S, Nysten B and Jonas A M 2005 Kinetics of exchange of alkanethiol monolayers self-assembled on polycrystalline gold *Langmuir* **21** 6825-9
[32] Tan Y S, Srinivasan M P, Pehkonen S O and Chooi S Y M 2006 Effects of ring substituents on the protective properties of self-assembled benzenethiols on copper Corros. Sci. 48 840-62
[33] Tatara S, Kuzumoto Y and Kitamura M 2016 Wettability control of gold surfaces modified with benzenethiol derivatives: Water contact angle and thermal stability *J. Nanosci. Nanotechnol.* **16** 3295-300
[34] Kim S H, Choi D, Chung D S, Yang C. Jang J, Park C H and Park S-H K 2008 High-performance solution-processed triisopropylsilylethynyl pentacene transistors and inverters fabricated by using the selective self-organization technique *Appl. Phys. Lett.* **93** 113306
[35] Lim J A, Lee W H, Kwak D and Cho K 2009 Evaporation-induced self-organization of inkjet-printed organic semiconductors on surface-modified dielectrics for high-performance organic transistors *Langmuir* **25** 5404-10
[36] Kang W, Kitamura M and Arakawa Y 2013 High performance inkjet-printed C_{60} fullerene thin-film transistors: Toward a low-cost and reproducible solution process *Organic Electron.* **14** 644-8
[37] Frisch M J, et al. 2010 Gaussian 09, Revision B.01 (Gaussian, Inc., Wallingford, CT)
[38] Lüth H 2001 Solid Surfaces Interfaces and Thin Films (Springer, Heidelberg) 4th edn chap 10
[39] Ikematsu N, Takahashi H, Hattori Y and Kitamura M 2019 Formation of a mixed monolayer on a gold surface using fluorobenzenethiol and alkanethiol *Jpn. J. Appl. Phys.* **59** SDDA09
[40] Schmidt C, Witt A and Witte G 2011 Tailoring the Cu(100) work function by substituted benzenethiolate self-assembled monolayers *J. Phys. Chem.* A **115** 7234-41
[41] Jia Z, Lee V W, Kymissis I, Floreano F, Verdini A, Cossaro A and Morgante A 2010 In situ study of pentacene interaction with archetypal hybrid contacts: Fluorinated versus alkane thiols on gold *Phys. Rev.* B **82** 125457
[42] Shi Z, Zhang Y, Liu M., Hanaor D and Gan Y 2018 Dynamic contact angle hysteresis in liquid bridges. *Colloids and Surfaces* A. **555** 365-71
[43] Owens D K 1969 Estimation of the surface free energy of polymers *J. Appl. Polym. Sci.* **13** 1741-7
[44] Shimizu R N and Demarquette N R 1999 Evaluation of surface energy of solid polymers using different models *J. Appl. Polym. Sci.* **76** 1831-45
[45] Gindl M, Sinn G, Gindl W, Reiterer A and Tschegg S 2001 A comparison of different methods to calculate the surface free energy of wood using contact angle measurements *Coll. Surf.* A **181** 279-87
[46] Yamamoto T and Takimiya K 2007 Facile synthesis of highly π-extended heteroarenes, dinaphtho[2,3-b:2',3'-f]chalcogenopheno[3,2-b]chalcogenophenes, and their application to field-effect transistors *J. Am. Chem. Soc.* **129** 2224-5
[47] Kitamura M, Kuzumoto Y, Kang W, Aomori S and Arakawa A 2010 High conductance bottom-contact pentacene thin-film transistors with gold-nickel adhesion layers *Appl. Phys. Lett.* **97** 033306